

Acceleration Harmonic Estimation and Suppression for Hydraulic Load Simulator Based on Artificial Bee Colony with Chaotic Search Strategy

Zhenshuai Wan^{1,2,*} – Longwang Yue² – Yanfeng Wang² – Pu Zhao²

¹ Henan University of Technology, Key Laboratory of Superhard Abrasives and Grinding Equipment, China

² Henan University of Technology, School of Mechanical and Electrical Engineering, China

This paper presents a new hybrid algorithm based on artificial bee colony (ABC) and chaotic search strategy (CSS), known as ABC-CSS to solve the harmonic estimation problems in the case of time varying acceleration response signal. The ABC algorithm simulates the intelligent behavior of bees in nature to find high-quality nectar sources according to different divisions of labor. Aiming at the lack of diversity, poor global and local search ability, as well as slow convergence speed of ABC, an improved ABC based on CSS is proposed. The algorithm generates new neighborhood points by the transformation of chaotic and decision variables by carrier mapping, which provides a broader search space and better location of nectar sources for bees and recruited observation bees, and enhances the diversity of bee colonies. At the same time, the investigation of a local honey bee search better solves the algorithm problem of the local minimum and improves the convergence property of the ABC. Simulation and experimental studies are conducted to validate the superiority of the proposed ABC-CSS in harmonic estimation.

Keywords: artificial bee colony, chaos-decision variable, harmonic distortion, harmonic estimation, harmonic suppression

Highlights

- The mathematical model of acceleration harmonic estimation is constructed.
- The chaotic search strategy is adopted to improve the global and local search ability as well as convergence speed of the artificial bee colony.
- The flowchart of the artificial bee colony and chaotic search strategy algorithm for acceleration harmonic estimation and elimination is proposed.
- The simulation and experiment results validate the harmonic estimation effectiveness of the artificial bee colony and chaotic search strategy.

0 INTRODUCTION

From simple parts to complicated equipment, vibration testing is required in the manufacturing process [1]. The purpose of vibration testing is to simulate the force and movement of equipment in the working process. Compared with field testing, load simulator testing under laboratory conditions is an indispensable part of product development and final mass production, and possesses the advantages of repeatability, low cost and safety [2]. As vibration environment simulation equipment, the load simulator can simulate sinusoidal, random, typical shock signal and self-set time domain waveform, such as the real load borne by the aircraft in the air [3], the structural stability of the car in the process of driving [4], and the seismic performance of large buildings under the excitation of seismic waves [5].

According to the drive types, load simulators are mainly divided into electric load simulators and hydraulic load simulators. Hydraulic load simulators are widely used in various industrial scenarios, such as exoskeleton robot and fatigue test devices due to their advantages of fast response, large load capacity

and high tracking accuracy. However, the inherent nonlinear characteristic and external disturbance of hydraulic system parameters result in the serious waveform distortion. Such waveform pollution may lead to adverse effects, such as the deterioration of vibration quality, the losses of vibrational energy, and structural failure. Thus, accurate harmonic parameter estimation is the first step to suppress waveform distortion [6].

To address the harmonic estimation problem, various methods have been proposed to estimate the amplitude and phase of harmonics. The fast Fourier transform (FFT) is widely used for stationary signal harmonic analysis, but aliasing, leakage, and picket fence phenomena restrict its application under time varying frequency condition [7]. As an important time-domain analysis tool, wavelet analysis overcomes the defect that FFT is completely localized in frequency domain and has no localization in time domain [8]. The orthogonal wavelet decomposition is carried out for the signals containing harmonics, and the multi-resolution concept is used to treat the results on the high scale as the fundamental component without harmonics. However, the algorithm needs

*Corr. Author's Address: Henan University of Technology, No. 100 Lianhua Street, Zhengzhou, China, wanzhenshuai@haut.edu.cn

software to realize the large amount of calculation, which influences the real-time performance and the estimation accuracy [9]. In addition, the real-time performance of wavelet analysis is difficult to guarantee, and the estimation accuracy is relatively low.

Recently, several intelligent optimization algorithms, such as simulated annealing (SA) [10], genetic algorithm (GA) [11], particle swarm optimization (PSO) [12], gravitational search algorithm (GSA) [13], and artificial bee colony (ABC) [14], have been applied to estimate the harmonic components presented in power system voltage waveforms. Bečirović et al. [10] developed SA to correctly estimate the harmonics state, where root mean square and angle values of voltage harmonics are used as important indexes to measure the identification accuracy. Milovanović et al. [11] presented the GA approach to mitigate harmonics in power distribution systems with linear and nonlinear loads, where the harmonic identification problem is converted to solve the multi-objective optimization problem with equality and inequality constraints. Waqas et al. [12] proposed the PSO method to estimate the harmonics polluted by time-varying noisy power signals, where PSO was hybridized with least square (LS) to effectively detect both the linear amplitude and nonlinear phases of harmonics. Singh et al. [13] discussed power system harmonic estimation based on the GSA with the aim of reduction of total harmonic distortion (THD) and improvement in waveform. The above-mentioned intelligent optimization methods have a parallel processing ability that enhances their search capability when applied to complex optimization problems [14]. Due to the fact that voltage signal is nonlinear in phase and linear in amplitude, phase of the harmonic components is obtained by using intelligent optimization method and the amplitude of the harmonic is acquired by LS [15]. The separation identification of amplitude and phase intensifies the complexity of the algorithm, which is not conducive to the real-time suppression of harmonics. In addition, Liu et al. [16] to [18] proposed improved ant colony optimization algorithm and multi-search strategy to solve many engineering problems including three-dimensional pipe routing design and path planning, which broadens the application of the intelligent optimization algorithm.

In recent years, ABC has been developed for solving the limited numerical optimization problem, neural network training, digital filter design and so on, which achieves good test results [19]. Biswas et al. [20] combined ABC and recursive least square

(RLS) to solve the harmonic estimation problems even that the number of harmonics is unknown. Hillis et al. [21] concluded that the ABC has better optimization performance than other intelligent optimization algorithms in iterative error curves by quantitative comparison and verification of various intelligent optimization algorithms. Zhou et al. [22] combined Markov property and convergence criterion of random search algorithm to prove the global convergence property of ABC. Chahkandi et al. [23] improved and optimized the ABC from three aspects: colony initialization, neighborhood search, and following behavior, to effectively balance global search and local search, where the adaptive learning mechanism is used to solve complex problems in different forms. In fact, the ABC algorithm obtains the optimal honey source by searching the location information, so neighborhood search is particularly important. At present, the improvement methods of ABC are mostly in convergence speed, which maybe miss a part of the neighborhood search range. What is more, the limitation of neighborhood search will directly lead to the reduction of bee colony diversity and a tendency to fall into a local optimal value [24]. It is possible to fail to find the global optimal solution for some special optimization problems. Therefore, an improved ABC, based on CSS, is proposed to estimate the harmonic information of hydraulic load simulator. The CSS enhances the diversity of population and improves the global search ability by introducing carrier mapping. Compared with other intelligent optimization algorithms, the proposed ABC-CSS has been proven to have faster convergence, higher capability to escape from local optima and obtain better quality of solutions. In addition, the proposed hybridized method gets better estimation performance and less computational burden in presence of noise components.

1 MATHEMATICAL MODEL OF ACCELERATION HARMONIC ESTIMATION

The sine acceleration response signal of a hydraulic load simulator is usually made up of a fundamental component plus some harmonic components and noise. Mathematically, the sine acceleration response can be modelled as the sum of sine or cosine functions with higher-order frequencies. Thus, the output of acceleration response can be represented as

$$a(t) = \sum_{n=1}^N A_n \sin(\omega_n t + \Phi_n) + v(t), \quad (1)$$

where $a(t)$ is the acceleration response signal; A_n , ω_n , Φ_n are amplitude, angular frequency and phase of n^{th} the harmonic component; v is measurement noise. The angular frequency is given as $\omega_n = 2\pi f_n = 2\pi n f_1$, where f_1 is the fundamental frequency.

The discrete model of the acceleration response can be expressed as

$$a(k) = \sum_{n=1}^N A_n \cos \Phi_n \sin(n\omega k) + A_n \sin \Phi_n \cos(n\omega k), \quad (2)$$

The parametric representation of acceleration response signal can be written as

$$a(k) = W(k)X(k), \quad (3)$$

Define $X_{n1} = A_n \cos \Phi_n$, $X_{n2} = A_n \sin \Phi_n$, then the harmonic vector $X(k)$ and parameter vector $W(k)$ are defined as

$$X(k) = \begin{bmatrix} \sin(\omega k), \cos(\omega k), \sin(2\omega k), \cos(2\omega k), \\ \dots, \sin(N\omega k), \cos(N\omega k) \end{bmatrix}^T, \quad (4)$$

$$W(k) = [x_{11}, x_{12}, x_{21}, x_{22}, \dots, x_{N1}, x_{N2}], \quad (5)$$

where the harmonic vector $X(k)$ is derived from the given reference frequency, the parameter vector $W(k)$ is updated by the proposed algorithm.

The estimation model of the acceleration response signal is given by

$$a(k) = \hat{a}(k) + e(k), \quad (6)$$

where $\hat{a}(k)$ is the estimation of $a(k)$, $e(k)$ denotes the estimation error.

The goal of harmonic estimation is that it will try to find the best value of $W(k)$ so that $e(k)$ becomes the minimum value. After obtaining the optimal value of parameter vector, the amplitudes and phases of the fundamental and n^{th} harmonic are derived as

$$\begin{cases} A_i = \sqrt{x_{n1}^2 + x_{n2}^2} \\ \Phi_i = \arctan(x_{n2} / x_{n1}) \end{cases}, \quad (7)$$

2 ACCELERATION HARMONIC ESTIMATION AND SUPPRESSION APPROACH BASED ON ABC-CSS

2.1 The Standard ABC

The basic steps of the ABC algorithm are as follows: The colony size is N_p , the employed bee size is N_e , the number of nectar sources is $N_p/2$, the dimension of the nectar source is D , the number of iterations is K , the threshold of bee retention is Limit, and the population of employed bees is $X = [X_1, X_2, \dots, X_{N_e}]$. Then the

randomly distributed initial population of N_p solutions is expressed as

$$X_i^j = X_{\min}^j + \text{rand}(0,1)(X_{\max}^j - X_{\min}^j), \quad (8)$$

where $i = \{1, 2, \dots, N_p\}$ and $j = \{1, 2, \dots, D\}$, X_{\max}^j and X_{\min}^j are the lower and upper bound of the solution variable X_i^j , respectively.

For the employed bees in step n , a new location is searched in the neighborhood of the current location vector, and the search formula is

$$\text{new_}X_i^j = X_i^j + \varphi_i^j (X_i^j - X_k^j), \quad (9)$$

where $j = \{1, 2, \dots, D\}$ and $k = \{1, 2, \dots, N_e\}$, $k \neq i$, k and j are random numbers of $[-1, 1]$.

According to the principle of optimal fitness selection, it is necessary to keep the optimal location of honey source and make the search direction of bee colony iterative in the direction of high honey source content. Then the probability distribution of new honey source search is represented as

$$\begin{aligned} P\{T_s(\mathbf{X}_i, \text{new_}\mathbf{X}_i) = \text{new_}\mathbf{X}_i\} \\ = \begin{cases} 1 & f(\text{new_}\mathbf{X}_i) \geq f(\mathbf{X}_i) \\ 0 & f(\text{new_}\mathbf{X}_i) < f(\mathbf{X}_i) \end{cases}, \end{aligned} \quad (10)$$

where \mathbf{X}_i is the current time honey source position vector, $\text{new_}\mathbf{X}_i$ is the new honey source position vector.

The probability that different onlooker bees are recruited as corresponding employed bees is

$$P\{T_s(X_i) = \mathbf{X}_i\} = \frac{f(\mathbf{X}_i)}{\sum_{m=1}^{N_e} f(X_m)}, \quad (11)$$

where T_s denotes stochastic mapping.

In the search process of nectar source, $\text{trail}(i)$ is constantly used to record the search times of the same honey bee for the same nectar source location. When $\text{trail}(i) > \text{Limit}$ and Eq. (10) is not satisfied, it means that the honey source in the neighborhood is generally low. If the honey source is searched here again, it will seriously affect the quality of honey source and search speed. So, it is necessary to re-specify the initial honey source location of such bees

$$\begin{aligned} X_i(n+1) = \\ \begin{cases} X_{\min} + \text{rand}(0,1)(X_{\max} - X_{\min}) & \text{trail}(i) \geq \text{Limit} \\ X_i(n) & \text{trail}(i) < \text{Limit} \end{cases}, \end{aligned} \quad (12)$$

If the stop criterion is met, the calculation is stopped and the optimal fitness value is obtained, then the number of iterations is increased by 1. Otherwise

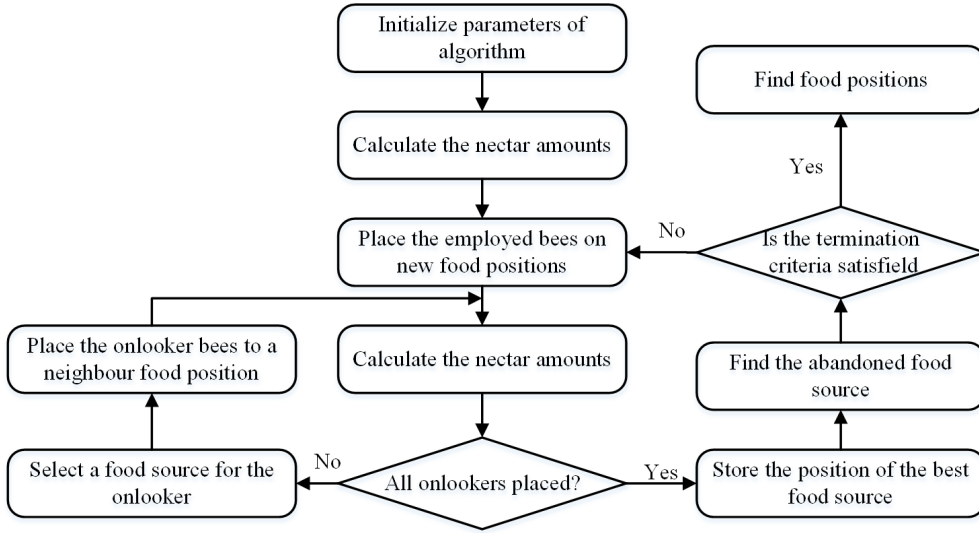


Fig. 1. The flowchart of the entire ABC algorithm

the iteration continues. The flowchart of the ABC algorithm is shown in Fig. 1.

2.2 The Improved ABC-CSS

In view of the lack of diversity, slow convergence speed and local optimum in the optimization process of ABC, an improved ABC based on CSS is introduced. In the improved method, the CSS is used to refine the search space of bee collecting and observing bees in the ABC algorithm, and a new neighborhood point of local optimal solution was generated in the iterative evolution, which accelerated the search of scout bees and made the bees find the optimal honey source at the fastest speed.

The chaotic search map can be expressed as

$$y_{n+1,d} = \mu y_{n,d} (1 - y_{n,d}), \quad (13)$$

where μ is the control parameter of chaotic state, $n=1, \dots, N_{max}$, $d=1, \dots, D$, and $y_{n,d}$ is the generated chaotic sequence.

According to the new neighborhood points of the local optimal solution, the chaotic variable is amplified by the carrier mode and applied to the single variable to be searched for honey source. The new variable is defined as

$$y'_{n,d} = f_{i,d} + R_{i,d} (2y_{n,d} - 1), \quad (14)$$

where $y'_{n,d}$ is the decision variable, $f_{i,d}$ is the center of honey source, and $R_{i,d}$ is the radius.

3 SIMULATION RESULTS

To validate the accuracy and convergence of the proposed ABC-CSS algorithm, a distorted waveform has been considered as a test signal, which includes six harmonics. In addition, several comparison algorithms are tested to validate the versatility of the developed method. The parameters are adjusted by trial-and-error method to ensure the good performance of the three controllers. The initialization parameters of ABC-CSS are $N_p=200$, $D=100$, $N_e=40$, $K=2000$, $Limit=100$, $\mu=4$, $R_{i,d}=0.2$. Fig. 2 shows the SA, GA, PSO, GSA, ABC and ABC-CSS, fitness against iteration times. It can be seen that the proposed ABC-CSS obtained the smallest fitness value in minimum iteration times.

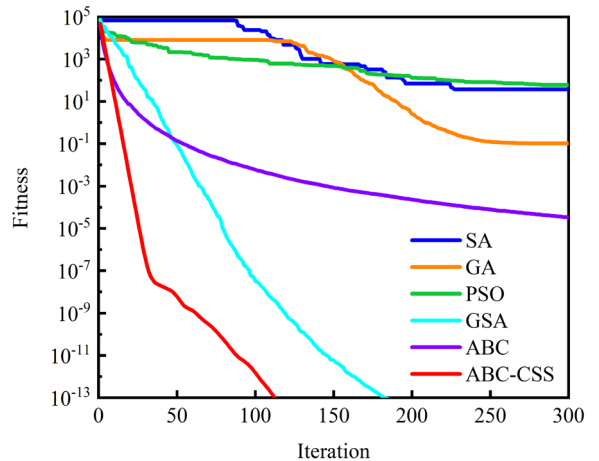


Fig. 2. The fitting curves of different algorithms

The detailed identification results are collected in Table 1. In order to ensure the fairness of the comparison, the experimental result is the average after 100 runs of each algorithm with different initial values. The harmonic parameters calculated by the proposed algorithm exhibit the best estimation accuracy, where the largest amplitude error is 0.3 %, which occurred at the 4th harmonic estimation. Besides, the standard deviation results indicate that the ABC-CSS method is the best performance among

the compared algorithms. The computation time of ABC-CSS is the smallest compared to the other five algorithms. To verify the performance of the proposed algorithm in solving local minima, Rosenbrock benchmark function is tested with six algorithms. As is shown in Fig. 3, the ABC-CSS has excellent performance in both convergence accuracy and convergence process.

Table 1. Comparison results of harmonic identification based on different algorithms

Algorithms	Parametres	Fund	2 nd	3 rd	4 th	5 th	6 th	Time [s]
Actual	Frequency [Hz]	5	10	15	20	25	30	15.2
	Amplitude [m/s ²]	6	5	4	3	2	1	
	Phase [rad]	-0.1	0.1	0.3	-0.3	0.7	-0.7	
SA	Amplitude [m/s ²]	5.876	4.897	3.921	2.935	1.957	0.981	13.4
	Error [%]	2.067	2.067	1.975	2.167	2.150	1.900	
	Std [m/s ²]	0.012	0.010	0.008	0.007	0.004	0.002	
	Phase [rad]	-0.092	0.091	0.287	-0.287	0.687	-0.685	
	Error [%]	8.000	9.000	4.330	4.300	1.857	2.143	
	Std [rad]	8E-4	9E-4	0.001	0.001	0.001	0.002	
	Amplitude [m/s ²]	5.898	4.905	3.945	2.942	1.961	0.985	
GA	Error [%]	1.700	1.900	1.375	1.933	1.950	1.500	12.6
	Std [m/s ²]	0.010	0.010	0.006	0.006	0.004	0.002	
	Phase [rad]	-0.094	0.093	0.291	-0.289	0.689	-0.689	
	Error [%]	6.000	7.000	3.000	3.667	1.571	1.571	
	Std [rad]	6E-4	7E-4	9E-4	0.001	0.001	0.001	
	Amplitude [m/s ²]	5.924	4.938	3.967	2.953	1.964	0.990	
PSO	Error (%)	1.267	1.240	0.825	1.567	1.800	1.00	11.2
	Std [m/s ²]	0.008	0.006	0.003	0.005	0.004	0.001	
	Phase [rad]	-0.095	0.095	0.293	-0.292	0.693	-0.692	
	Error [%]	5.000	5.000	2.333	2.667	1.000	1.142	
	Std [rad]	5E-4	5E-4	7E-4	8E-4	7E-4	8E-4	
	Amplitude [m/s ²]	5.958	4.956	3.978	2.963	1.968	0.992	
GSA	Error [%]	0.700	0.880	0.55	1.233	1.600	0.800	10.5
	Std [m/s ²]	0.004	0.004	0.002	0.004	0.003	8E-4	
	Phase [rad]	-0.097	0.097	0.295	-0.295	0.694	-0.695	
	Error [%]	3.000	3.000	1.667	1.667	0.857	0.714	
	Std [m/s ²]	3E-4	3E-4	5E-4	5E-4	6E-4	5E-4	
	Amplitude [m/s ²]	5.984	4.987	3.997	2.967	1.987	0.995	
ABC	Error [%]	0.267	0.260	0.075	1.100	0.650	0.500	9.7
	Std [rad]	0.002	0.001	3E-4	0.003	0.001	5E-4	
	Phase [rad]	-0.098	0.098	0.298	-0.297	0.695	-0.697	
	Error [%]	2.000	2.000	0.667	1.000	0.714	0.429	
	Std [m/s ²]	2E-4	2E-4	2E-4	3E-4	5E-4	3E-4	
	Amplitude [m/s ²]	5.999	4.992	4.001	2.991	2.003	0.999	
ABC-CSS	Error [%]	0.017	0.160	0.025	0.300	0.150	0.100	6.5
	Std [m/s ²]	1E-4	8E-4	1E-4	9E-4	3E-4	1E-4	
	Phase [rad]	-0.099	0.099	0.299	-0.298	0.699	-0.699	
	Error [%]	1.000	1.000	0.330	0.667	0.143	0.143	
	Std [rad]	1E-4	1E-4	1E-4	2E-4	1E-4	1E-4	

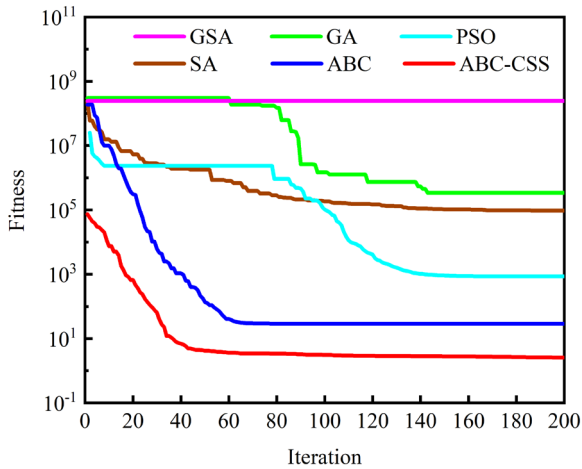


Fig. 3. The fitting curves of Rosenbrock function

The inherent nonlinear factors of the servo system cause serious harmonic distortion of the load simulator sinusoidal acceleration response. The adaptive notch filter can suppress the harmonic of the acceleration response signal in real time, so as to significantly

improve the reliability of the load simulator's sinusoidal acceleration test. The flowchart of ABC-CSS algorithm for acceleration harmonic estimation and suppression is shown in Fig. 4, where r and a are reference signal and response signal, respectively. The amplitude and phase information of harmonics are estimated by the ABC-CSS algorithm based on the acceleration response. The adaptive notch filter generates a signal with the frequency of harmonic that should be eliminated from the acceleration response, where the centre frequency is determined by reference acceleration signal.

Fig. 5 shows the estimation amplitude and phase of each harmonic. It is noted that the amplitude and phase reach the given parameters after 0.4 s, which shows the fast convergence of the proposed algorithm. In addition, 5 dB, 10 dB, 15 dB and 20 dB gaussian noise are conducted to validate the estimation accuracy and robustness of the proposed algorithm. The harmonic amplitude and phase results under different SNR (signal-to-noise ratios) are shown in Fig. 6. These results demonstrate that the ABC-

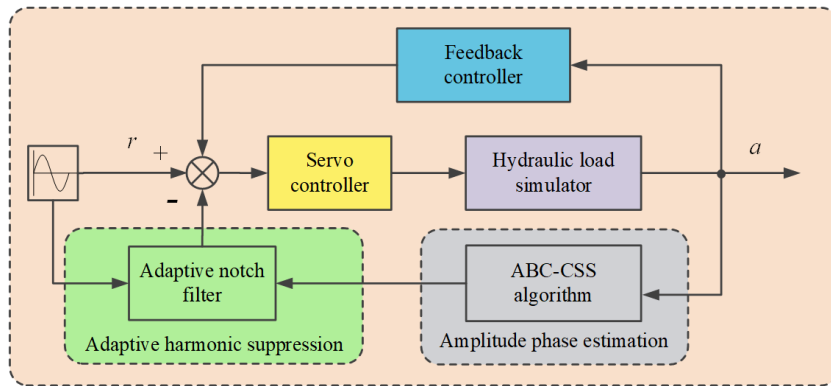


Fig. 4. Flowchart of ABC-CSS algorithm for acceleration harmonic estimation and elimination

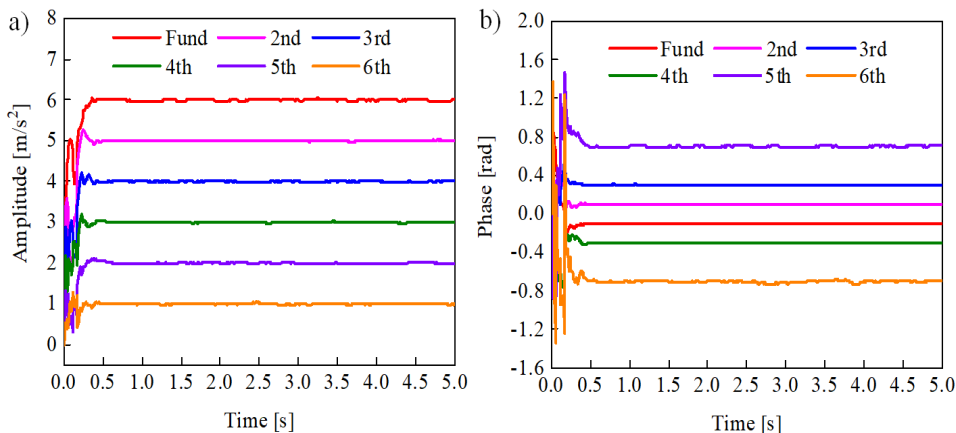


Fig. 5. The estimation amplitude and phase of each harmonic; a) amplitude, and b) phase

Uncorrected proof

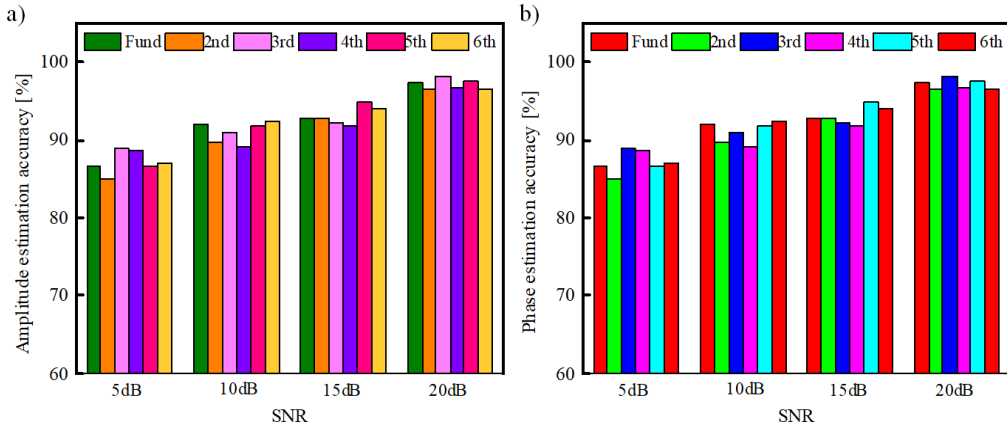


Fig. 6. The estimation harmonic amplitude and phase under noise; a) amplitude, and b) phase

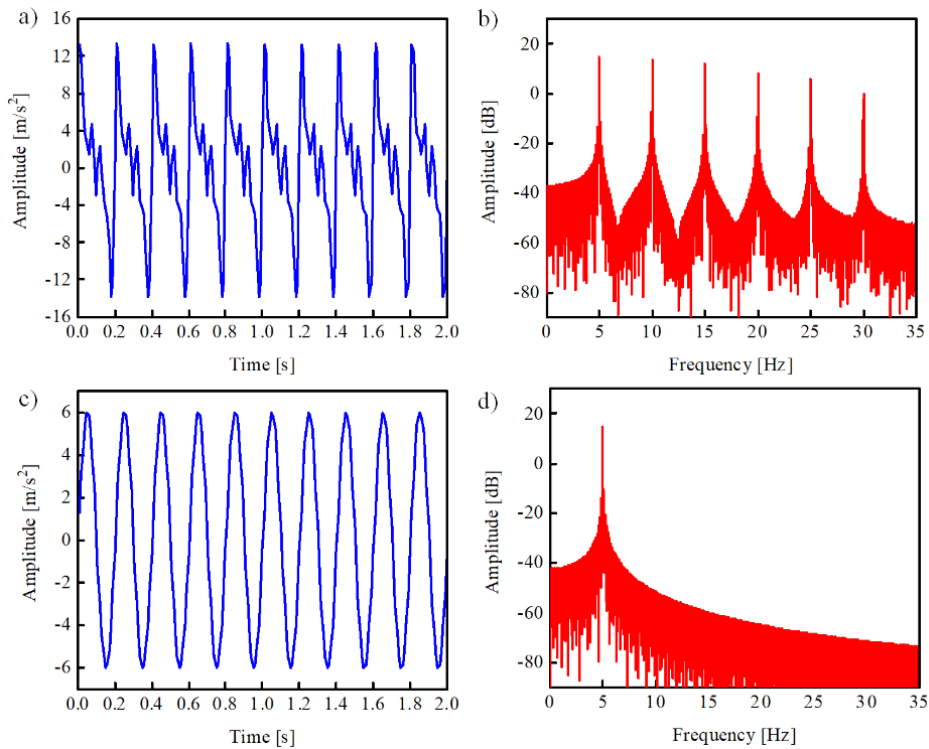


Fig. 7. Time domain and frequency domain response before and after harmonic suppression; a) the time domain before elimination, b) the frequency domain before elimination, c) the time domain after elimination, and d) the frequency domain after elimination

Uncorrected proof

CSS has good anti-interference performance in the estimation of each harmonic component containing noise component. Fig. 7 gives the time domain and frequency domain response results before and after harmonic suppression. The results show that the distortion of the sinusoidal acceleration signal is obviously improved after the harmonic suppression, and the response signal can reproduce the given reference signal well.

4 EXPERIMENTAL RESULTS

An experimental system of the hydraulic load simulator is shown in Fig. 8, which includes controller module, servo valve, sensor system and hydraulic system. The proposed algorithm is coded by MATLAB/Simulink and compiled by Microsoft Visual Studio.NET. The hydraulic valve drives the load simulator movement, where the control signal is processed by control

module. The position signal and pressure signal of the load simulator are measured by corresponding sensors and then transmitted to the controller and finally fed back to the computer. The hydraulic valve converts the hydraulic energy of the hydraulic system into the working force of the hydraulic cylinder according to the flow rate of the oil source, so as to drive the load simulator to produce the desired movement. It should be noted that the mechanical and hydraulic parameters are changed in real time during the experiment.

The time domain response and frequency domain response of low-frequency acceleration signal $y(t)=4\sin(2\pi t)$ [m/s²] are shown in Fig. 9. It can be seen from the time domain response that the distortion of the acceleration response signal is relatively serious, and the frequency domain response indicates the acceleration signal is contaminated by higher order harmonic components. The amplitude and phase estimated by the proposed method of each harmonic is shown in Fig. 10. It can be seen that the convergence speed of the identification result is very fast, the amplitude and phase converge to the stable state within 2 s, and the identification precision of the

amplitude is higher than that of the phase. Specially, the fundamental amplitude is the largest, and the other harmonic amplitudes are relatively smaller. It can be seen from the identification amplitude that the fifth harmonic component in the acceleration response is large, so the influence of the fifth harmonic on the waveform distortion should be suppressed first. The sinusoidal acceleration response after adopting the adaptive harmonic suppression strategy is shown in Fig. 11. It can be seen from the time-domain response that the waveform distortion of the acceleration response signal is greatly improved after suppressing the fifth harmonic. Compared with the frequency domain response before and after harmonic suppression, it can be seen that the amplitude decreases by 30 dB after the fifth harmonic suppression. The THD analysis results before and after harmonic suppression are collected in Table 2, in which it can be seen that the amplitude of the fifth harmonic drops sharply from 0.364 m/s² before harmonic suppression to 0.006 m/s² after harmonic suppression, and the THD value drops from 14.17 % to 5.23 %.

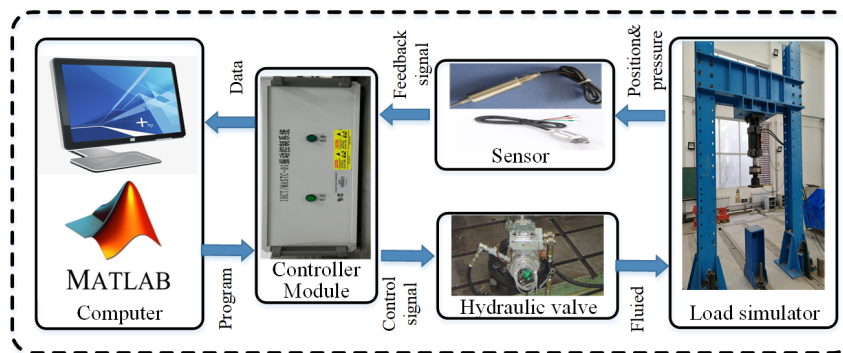


Fig. 8. Hydraulic load simulator system

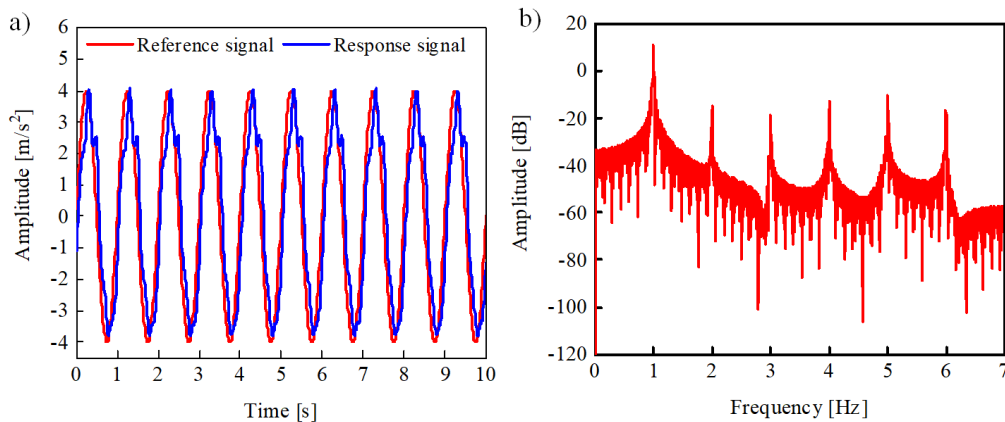


Fig. 9. Time domain and frequency domain response; a) time domain, and b) frequency domain

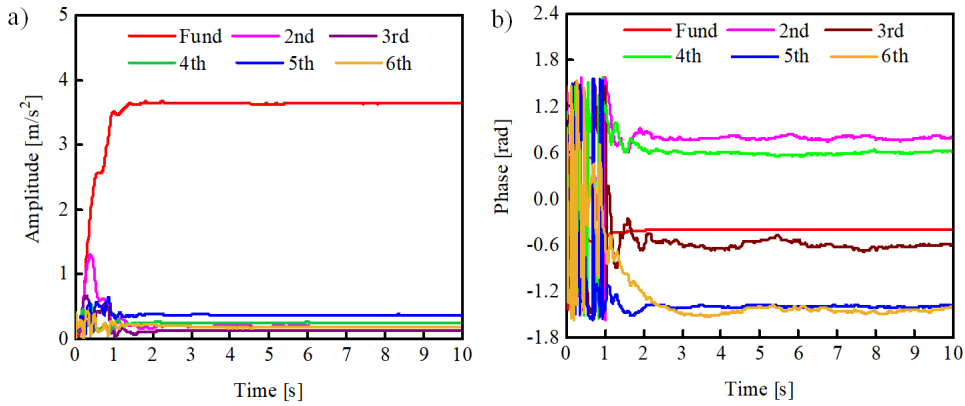


Fig. 10. Estimated amplitude and phase; a) amplitude, and b) phase

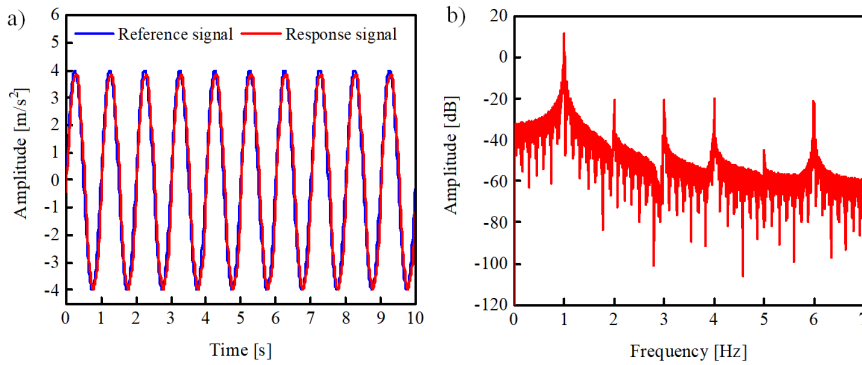


Fig. 11. Acceleration response after harmonic suppression; a) time domain, and b) frequency domain

Table 2. THD analysis results of $y(t) = 4\sin(2\pi t)$

Harmonic	Before suppression	After suppression
Fund	3.642	3.984
2nd	0.185	0.098
3rd	0.124	0.101
4th	0.245	0.112
5th	0.364	0.006
6th	0.172	0.105
THD [%]	14.17	5.23

Fig. 12 shows the time and frequency domain responses of the sinusoidal input signal of $y(t) = 6\sin(8\pi t)$ [m/s²]. It can be seen from the time-domain response that there are amplitude attenuation and phase lag in the response signal to some extent, and especially the distortion at the crest and trough is serious. The frequency domain response shows that the amplitude of the 5th harmonic is the largest; the 3rd harmonic is the smallest. Thus, suppressing the 5th harmonic is helpful to improve the waveform reproduction accuracy of the desired sinusoidal input signal. The identified harmonic amplitude and phase are shown in Fig. 13. It can be seen from the figure

that the identification speed of amplitude and phase is very fast, and it only takes 0.4 s to accurately identify the amplitude and phase information of each harmonic.

The time domain and frequency domain responses of the sine acceleration after the suppression of the 5th harmonic are shown in Fig. 14. From the time domain diagram, it can be seen that the response signal after the suppression of the 5th harmonic fits the input signal well. It can be seen from the frequency domain response diagram that the higher harmonics all decrease to some extent, which indicates that the harmonic suppression strategy based on adaptive notch filter can weaken the 5th harmonic in the response signal well. The THD analysis results before and after harmonic suppression are shown in Table 3. It can be seen that THD decreases by nearly 13.3 % after the fifth harmonic suppression, which indicates that the waveform distortion is greatly improved. The acceleration response after harmonic suppression can reproduce the given time domain reference signal well and accurately simulate the expected sinusoidal motion.

Uncorrected proof

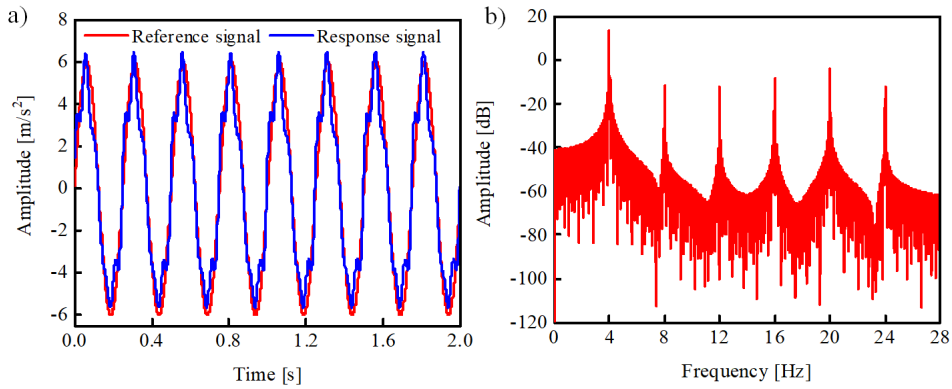


Fig. 12. Time and frequency domain response; a) time domain e, and b) frequency domain

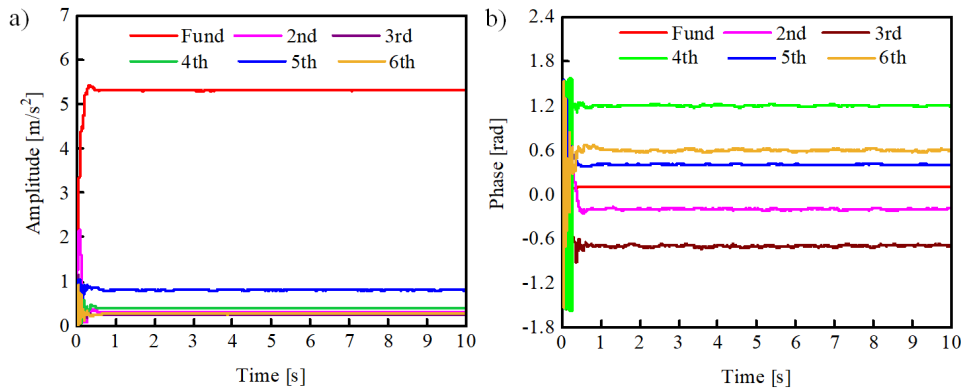


Fig. 13. Estimated amplitude and phase; a) amplitude, and b) phase

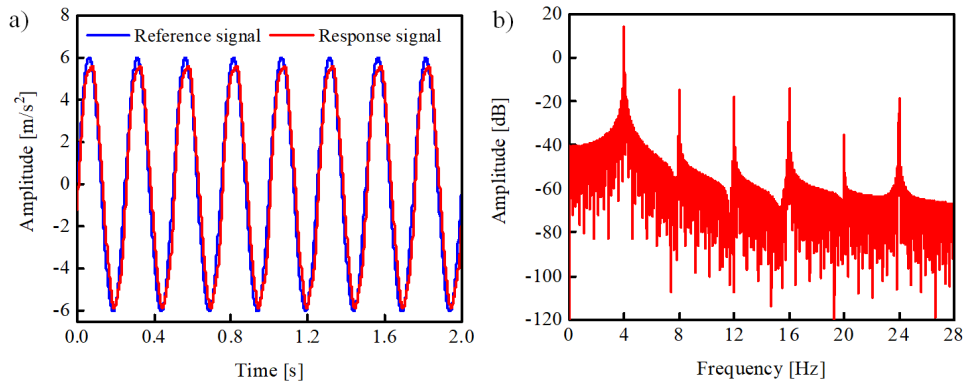


Fig. 14. Acceleration response after harmonic suppression; a) time domain, and b) frequency domain

Table 3. THD analysis results of $y(t) = 5\sin(8\pi t)$

Harmonic	Before suppression	After suppression
Fund	5.321	5.797
2nd	0.313	0.212
3rd	0.245	0.131
4th	0.407	0.198
5th	0.811	0.021
6th	0.271	0.124
THD [%]	19.30	5.91

5 CONCLUSIONS

This paper developed an ABC-CSS method to accurately estimate the amplitude and phases of acceleration response contaminated with nonlinear factors and disturbances. In this hybrid algorithm, the chaotic search strategy is introduced to map the value of chaos variable to the value range of the optimization variable by the carrier mode. The new

neighborhood points of the local optimal solution are generated, which speeds up the global search ability and local search ability, enhances the diversity of bee colonies, and improves the convergence speed of the algorithm. Simulation and experiments were conducted to verify the effectiveness of the harmonic information estimation including amplitude and phase. The harmonic suppression strategy based on an adaptive notch filter neither needs to identify the model of the system, nor to be targeted at specific kinds of non-linear factors, so it has strong universality and practical application. In addition, simple structure and less computation can ensure the real-time on-line harmonic suppression.

6 ACKNOWLEDGEMENTS

This research was funded by the Henan Key Laboratory of Superhard Abrasives and Grinding Equipment, Henan University of Technology (JDKFJJ2023005), the Key Science and Technology Program of Henan Province (242102221001, 232102220085).

7 REFERENCES

- [1] Zhu, L.K., Wang, Z.B., Qiang, H., Liu, Y.Q. (2019). Global sliding-mode dynamic surface control for MDF continuous hot-pressing slab thickness via LESO. *International Journal of Machine Learning and Cybernetics*, vol. 10, p. 1249-1258, DOI:10.1007/s13042-018-0804-y.
- [2] Guo, K., Li, M., Shi, W., Pan, Y. (2022). Adaptive tracking control of hydraulic systems with improved parameter convergence. *IEEE Transactions on Industrial Electronics*, vol. 69, no. 7, p. 7140-7150, DOI:10.1109/tie.2021.3101006.
- [3] Xu, Z., Liu, Q., Yao, J. (2021). Adaptive prescribed performance control for hydraulic system with disturbance compensation. *International Journal of Adaptive Control and Signal Processing*, vol. 35, no. 8, p. 1544-1561, DOI:10.1002/acs.3262.
- [4] Dahunsi, O.A., Pedro, J.O., Nyandoro, O.T. (2010). System identification and neural network based pid control of servo-hydraulic vehicle suspension system. *SAIEE Africa Research Journal*, vol. 101, no. 3, p. 93-105, DOI:10.23919/SAIEE.2010.8531554.
- [5] Jing, C.H., Xu, H.G., Jiang, J.H. (2019). Flatness-based adaptive nonlinear control for torque tracking of electro-hydraulic friction load simulator with uncertainties. *Proceedings of the Institution of Mechanical Engineers, Part I; Journal of Systems and Control Engineering*, vol. 233, no. 8, p. 1009-1016, DOI:10.1177/0959651818813230.
- [6] Dong, L., Wei, X., Zhang, H. (2019). Anti-disturbance control based on nonlinear disturbance observer for a class of stochastic systems. *Transactions of the Institute of Measurement and Control*, vol. 41, no. 6, p. 1665-1675, DOI:10.1177/0142331218787608.
- [7] Zhang, Z., Gu, C., Xuan, X. (2024). A transistor-based high-efficiency rectifier using input second harmonic component. *IEEE Transactions on Circuits and Systems I: Regular Papers*, vol. 71, no. 1, p. 110-119, DOI:10.1109/tcsi.2023.3331155.
- [8] Shahroudi, M.M., Faghihi, F., Mozafari, B. (2023). A novel control scheme for load current components sharing improvement, and unbalanced and harmonic voltage compensation, in islanded provisional-microgrids. *Electric Power Systems Research*, vol. 223, 109560, DOI:10.1016/j.epsr.2023.109560.
- [9] Tapia-Olvera, R., Guillen, D., Beltran-Carbajal, F., Castro, L.M. (2022). An adaptive scheme to improve prony's method performance to estimate signal parameters of power system Oscillations. *IEEE Transactions on Instrumentation and Measurement*, vol. 71, 9005212, DOI:10.1109/tim.2022.3191721.
- [10] Becirović, V., Pavić, I., Filipović-Grčić, B. (2018). Sensitivity analysis of method for harmonic state estimation in the power system. *Electric Power Systems Research*, vol. 154, p. 515-527, DOI:10.1016/j.epsr.2017.07.029.
- [11] Milovanović, M., Radosavljević, J., Klimenta, D., Perovic, B. (2019). GA-based approach for optimal placement and sizing of passive power filters to reduce harmonics in distorted radial distribution systems. *Electrical Engineering*, vol. 101, p. 787-803, DOI:10.1007/s00202-019-00805-w.
- [12] Waqas, A.B., Saifullah, Y., Ashraf, M.M. (2021). A Hybrid quantum inspired particle swarm optimization and least square framework for real-time harmonic estimation. *Journal of Modern Power Systems and Clean Energy*, vol. 9, no. 6, p. 1548-1556, DOI:10.35833/mpce.2019.000098.
- [13] Singh, S.K., Kumari, D., Sinha, N., Goswami, A.K., Sinha, N. (2017). Gravity search algorithm hybridized recursive least square method for power system harmonic estimation. *Engineering Science and Technology, an International Journal*, vol. 20, no. 3, p. 874-884, DOI:10.1016/j.jestch.2017.01.006.
- [14] Cao, J., Yin, B., Lu, X., Kang, Y., Chen, X. (2018). A modified artificial bee colony approach for the 0-1 knapsack problem. *Applied Intelligence*, vol. 48, p. 1582-1595, DOI:10.1007/s10489-017-1025-x.
- [15] Boudardara, F., Gorkemli, B. (2020). Solving artificial ant problem using two artificial bee colony programming versions. *Applied Intelligence*, vol. 50, p. 3695-3717, DOI:10.1007/s10489-020-01741-0.
- [16] Liu, C., Wu, L., Li, G., Zhang, H., Xiao, W., Xu, D., Guo, J., Li, W. (2024). Improved multi-search strategy A* algorithm to solve three-dimensional pipe routing design. *Expert Systems with Applications*, vol. 240, 122313, DOI:10.1016/j.eswa.2023.122313.
- [17] Liu, C., Wu, L., Xiao, W., Li, G., Xu, D., Guo, J., Li, W. (2023). An improved heuristic mechanism ant colony optimization algorithm for solving path planning. *Knowledge-Based Systems*, vol. 271, 110540, DOI:10.1016/j.knsys.2023.110540.
- [18] Liu, C., Wei, L., Huang, X., Xiao, W. (2022). Improved dynamic adaptive ant colony optimization algorithm to solve pipe routing design. *Knowledge-Based Systems*, vol. 237, 107846, DOI:10.1016/j.knsys.2021.107846.

- [19] Xiao, W., Li, G., Liu, C., Tan, L. (2023). A novel chaotic and neighborhood search-based artificial bee colony algorithm for solving optimization problems. *Scientific Reports*, vol. 13, 20496, DOI:10.1038/s41598-023-44770-8.
- [20] Biswas, S., Chatterjee, A., Goswami, S.K. (2013). An artificial bee colony-least square algorithm for solving harmonic estimation problems. *Applied Soft Computing*, vol. 13, no. 5, p. 2343-2355, DOI:10.1016/j.asoc.2012.12.006.
- [21] Hillis, A.J., Yardley, J., Plummer, A.R., Brask, A. (2020). Model predictive control of a multi-degree-of-freedom wave energy converter with model mismatch and prediction errors. *Ocean Engineering*, vol. 212, 107724, DOI:10.1016/j.oceaneng.2020.107724.
- [22] Zhou, Y., Ding, F. (2024). A novel recursive multivariate nonlinear time-series modeling method by using the coupling identification concept. *Applied Mathematical Modelling*, vol. 127, p. 571-587, DOI:10.1016/j.apm.2023.10.038.
- [23] Chahkandi, V., Yaghoobi, M., Veisi, G. (2013). CABC-CSA: a new chaotic hybrid algorithm for solving optimization problems., *Nonlinear Dynamics*, vol. 73, p. 475-484, DOI:10.1007/s11071-013-0802-2.
- [24] Korkmaz Tan, R., Bora, S. (2020). Adaptive modified artificial bee colony algorithms (AMABC) for optimization of complex systems. *Turkish Journal of Electrical Engineering and Computer Sciences*, vol. 28, no. 5, p. 2602-2629, DOI:10.3906/elk-1909-12.